

Phase Equilibria in the System between NbO_2 and Nb_2O_5 at High Temperatures

KEIJI NAITO, NAOKI KAMEGASHIRA,¹ AND NORIO SASAKI

Department of Nuclear Engineering, Faculty of Engineering, Nagoya University, Furo-cho, Chikusa-ku, Nagoya, Japan

Received October 15, 1979; in revised form January 31, 1980

Isothermal electrical conductivity measurements on niobium oxides were carried out over the temperature range from 1010 to 1300°C as a function of oxygen partial pressure in order to clarify the phase relations. Existence regions of the intermediate oxide phases between NbO_2 and Nb_2O_5 were found from the discontinuities in electrical conductivity curves. These oxide phases were also analyzed by gravimetric method and by X-ray diffractometry. From these results the phase diagram for this system is proposed. The defect structures of these phases are also discussed.

Introduction

Phase equilibria in the Nb-O system have been studied by many authors (1-14), and several oxide phases have been reported to exist between NbO_2 and Nb_2O_5 . The phases reported in the previous papers are summarized in Table I. As shown in the table, the existence range of these intermediate compounds is confused, especially in the temperature range 1000-1200°C.

In the present paper, the electrical conductivity of niobium oxides was measured under controlled oxygen partial pressures (from 10^5 to 10^{-15} Pa) in the temperature range 1010-1300°C, in order to clarify the phase relation and the existence regions of oxides in the NbO_2 - Nb_2O_5 system.

¹ Present address: School of Materials Science, Toyohashi University of Technology, Tempaku-cho, Toyohashi, 440 Japan.

Experimental

1. Apparatus and Measurement

Electrical conductivity measurements were carried out after equilibrating sample pellets at constant oxygen partial pressures. Temperature was measured by Pt-Pt13%Rh thermocouples. The electrical conductivity of the pellet was measured by the usual four probe method (15). The equilibration time during the electrical conductivity measurement ranged from 5 to more than 20 hr, depending on temperature and oxide phase. The measurements were repeated several times from higher to lower and lower to higher oxygen partial pressures and the existence of the equilibria was confirmed.

2. Control and Measurement of Oxygen Partial Pressure

Mixtures of Ar and O_2 gases were used

TABLE I
PHASES REPORTED BY THE PREVIOUS STUDIES FOR THE SYSTEM BETWEEN NbO₂ AND Nb₂O₅

Existence phase	<i>T</i> (°C)	Method ^a	Reference
Nb ₂ O ₅ (<i>x</i> = 0–0.1)	1350–1450	X	1
NbO _{2.40} , NbO _{2.46} , NbO _{2.48}	1150	X	3
Nb ₂ O _{5-x} (<i>x</i> = 0–0.079)	1090	EC, TG, I	2
<i>x</i> = 0–0.056)	889		
NbO _{2.454–2.474}	1100–1200	Q, X	4
Nb ₂ O _{5-x}	900–1200	R	13
NbO _{2.454–2.479} , NbO _{2.45} , NbO _{2.432}	1250	Q, X	5, 6
Nb ₁₂ O ₂₉ , Nb ₂₂ O ₅₄ , Nb ₄₇ O ₁₁₆ , Nb ₂₄ O ₆₂ , Nb ₅₃ O ₁₃₂	1300	Q, X	7
Nb ₁₂ O ₂₉ , Nb ₂₂ O ₅₄ , Nb ₄₇ O ₁₁₆ , Nb ₂₄ O ₆₂ , Nb ₅₃ O ₁₃₂	1300, 1400	Q, X	8
From NbO _{2.42} to NbO _{2.50} (coherent intergrowth)	900–1050	ED, EM	9
NbO _{2.42} , NbO _{2.47}	900–1100	TG, R	10–12
Some intermediate phases	900–1300	TG, R	14

^a X, X Ray; EC, electrochemical cell; TG, thermogravimetry; I, isopiestic; Q, quenching; R, electrical resistance; ED, electron diffraction; EM, electron microscopy.

for controlling higher oxygen partial pressures (10⁵–1 Pa) and H₂ and CO₂ gases for lower oxygen partial pressures (<1 Pa). The mixing ratio of the gases was determined by measuring the flow rate of each gas with a calibrated capillary-type flow meter. For mixtures of H₂ and CO₂, the oxygen partial pressures were calculated from the mixing ratio and the temperature using the JANAF thermodynamic table (16). Hydrogen and CO₂ gases were purified by removing oxygen with activated copper and then water with cold traps. The mixed gas was passed through a long furnace more than 50 cm with appropriate linear velocity to reach the equilibrium and the attainment to the equilibrium in the mixed gas in the furnace was confirmed preliminarily. Oxygen partial pressure higher than 10⁻⁷ Pa was also checked by measuring the electrical resistance of Co_{1-x}O (17), which was placed in another furnace. The fluctuations in the oxygen partial pressures lower than about 10⁻⁷ Pa

were monitored by measuring the electrical resistance of TiO_{2-x} (13, 17, 18) placed near the niobium oxide sample in the same furnace.

3. Samples

Nb₂O₅ powder (99.9% purity) was pressed into pellets of 7 mm diameter, then sintered in air at 1300–1340°C for about 3 days. The main impurities of Nb₂O₅ powder were Fe, Si, Ta, Al, Cr, Mn, Ti, Mo, and Ni. The sintered samples had densities of about 85% of the theoretical.

4. Analysis

The oxygen content of the quenched samples was determined from weight gain by oxidizing to stoichiometric Nb₂O₅ in air at 1000°C. The error in determining the O/Nb ratio was within ±0.002.

The sample composition was also determined continuously by a thermogravimetric technique using an automatic electromicro balance at 1060°C in the range of oxygen

partial pressure 10^5 – 10^{-9} Pa, where both the sample pellet for measuring the electrical conductivity and the TiO_2 wire for monitoring the oxygen partial pressure were placed very near the specimen in the thermal balance in order to carry out the measurements simultaneously. The phases existing in the sample at high temperatures were identified with use of X-ray diffractometry (19–24) after quenching the samples, but it was difficult to identify each phase clearly by the usual X-ray diffractometry because each phase shows a very similar pattern.

Results and Discussion

1. Isothermal Electrical Conductivity of Niobium Oxides

The dependences on oxygen partial pressures of the isothermal electrical conductivity of niobium oxides at 1010, 1060, 1110, 1200, and 1300°C are shown in Fig. 1.

As seen from the figures, the electrical conductivity increases with decreasing oxygen partial pressure at each temperature and becomes independent of P_{O_2} at lower partial pressures. This independent of P_{O_2} region was identified as the NbO_2 phase by chemical and X-ray analysis of the quenched samples (Fig. 2).

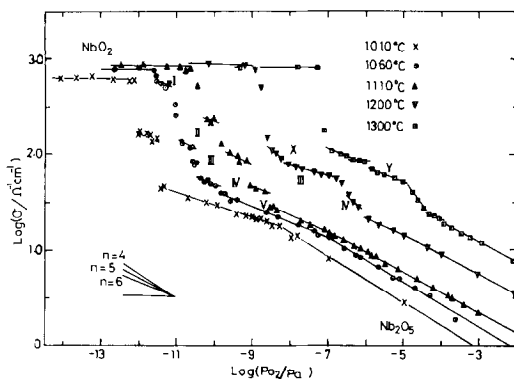


FIG. 1. Isothermal electrical conductivity of niobium oxides as a function of oxygen partial pressures.

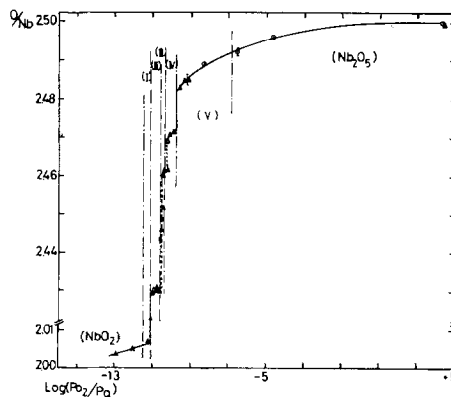


FIG. 2. Dependence of composition on oxygen partial pressure at 1060°C. $-\Delta-$, Quenching method; \odot , thermal balance; $-\cdot-\cdot-$, boundary obtained from electrical conductivity measurement.

At each temperature there exist some breaks and discontinuities in the electrical conductivity which suggest the presence of phase changes. The intermediate regions divided by these breaks or discontinuities are designated temporarily as I, II, III, IV, and V counting from the lower oxygen partial pressure region at 1060°C, as shown in Fig. 1, taking into account the chemical potential diagram (Fig. 4), as described in later section.

At 1110°C, the regions corresponding to II, III, IV, and V remain clearly, and at 1200°C a new region, designated as X, appears between II and III. At 1300°C another new region, designated as Y, appears between III and IV. The identification of each phase is described in the next section.

All intermediate regions between Nb_2O_5 and NbO_2 show n -type semiconductivity since the slopes of dependence of electrical conductivity on P_{O_2} are negative.

2. Composition of the Phases

Figure 2 shows the dependence of compositions on oxygen partial pressure at 1060°C. The numbers quoted in Fig. 2 indicate the regions named by the electrical conductivity measurement. As seen from

the figure, no discontinuous point is found in the region between Nb_2O_5 and V. Assuming that the $\text{Nb}_2\text{O}_{5-x}$ phase extends to the jump point between V and IV, the limiting composition of oxygen-deficient Nb_2O_5 is found to be $\text{NbO}_{2.484}$. The composition of phase IV is determined to be in the range from $\text{NbO}_{2.469}$ to $\text{NbO}_{2.472}$. Phase III has a narrow existence region of oxygen partial pressure at 1060°C and the composition is from $\text{NbO}_{2.460}$ to $\text{NbO}_{2.462}$. The composition of phase II is from $\text{NbO}_{2.430}$ to $\text{NbO}_{2.431}$ and that of I is $\text{NbO}_{2.007}$.

The dependence of composition on oxygen partial pressure at 1110°C is also shown in Fig. 3, where the composition of each phase was measured at the middle of the oxygen partial pressure existence region which was determined by electrical conductivity measurement. The Nb_2O_5 phase seems to extend to the region of V even at 1110°C . The existence of phase I which is suggested from the electrical conductivity measurement at 1060°C is doubtful.

3. Phase Relation

Logarithms of the boundary oxygen partial pressures obtained from the electrical conductivity measurement are plotted against reciprocal temperature in Fig. 4.

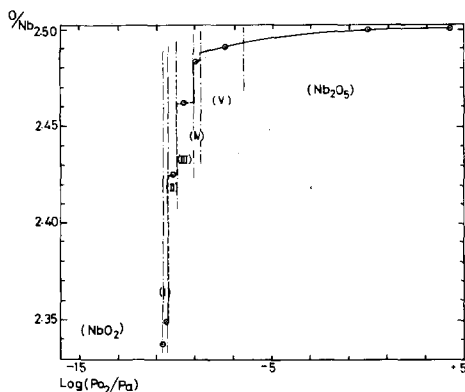


FIG. 3. Dependence of composition on oxygen partial pressure at 1110°C . —, Boundary obtained from electrical conductivity measurement.

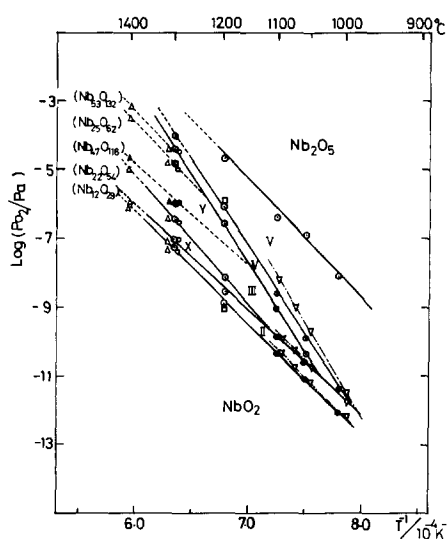


FIG. 4. Logarithms of boundary oxygen partial pressures obtained from the electrical conductivity measurement against reciprocal temperature. \circ , Schäfer *et al.* (1969); Δ , Kimura (1973); \square , Wimmer and Tripp (1973); ∇ , Marucco (1974); \odot , this work.

Data reported by other authors are also shown in this figure.

Based on this chemical potential diagram and the results of compositional determination together with X-ray analysis, the following conclusions can be made:

(a) Phase II may correspond to phase $\text{NbO}_{2.42}$ reported by Marucco (10) at 1000 – 1100°C and $\text{Nb}_{12}\text{O}_{29}$ reported by Schäfer *et al.* (7) at 1300°C and the same by Kimura (8) at 1300 and 1400°C . The X-ray diffraction pattern of phase II is in agreement with that of $\text{Nb}_{12}\text{O}_{29}$ (monoclinic) by Gruehn and Norin (19, 23).

(b) The existence regions of phases III and IV are clearly demonstrated in this study, while Marucco (10, 11) reported the existence of a single phase $\text{NbO}_{2.47}$ in this region. Phase III is considered to correspond to $\text{Nb}_{47}\text{O}_{116}$ reported by Schäfer *et al.* (7) and Kimura (8). X-Ray diffraction patterns of phase III are in fair agreement with those of $\text{NbO}_{2.464}$ by Gruehn and Norin (19, 23).

(c) Phases X and Y may correspond to Nb₂₂O₅₄ and Nb₂₅O₆₂, respectively.

(d) Phase IV nearly corresponds to NbO_{2.483} reported by Gruehn and Norin (19) or to Nb₅₃O₁₃₂ by Schäfer *et al.* (7) and Kimura (8), but the extrapolation of the boundary line between phases IV and V to higher temperatures in the chemical potential diagram suggests that phase IV may exist in the higher oxygen partial pressure region than that of Nb₅₃O₁₃₂ reported by Schäfer *et al.* and Kimura. Therefore Nb₅₃O₁₃₂ is likely to exist only at the temperature range higher than about 1230°C and is different from the phase IV as shown in Fig. 4.

(e) The extrapolation of the boundary line between phases IV and Nb₅₃O₁₃₂ to a higher temperature region suggests the existence of one more phase between them.

(f) Although region V is observed from the electrical conductivity measurement at 1010 to 1200°C, no difference in X-ray analysis between phases V and Nb₂O₅ was found and no discontinuity in the dependence of O/Nb ratio on oxygen partial pressures was observed. Therefore phase V is considered to be the region where the different kinds of defects are formed within the Nb₂O₅ phase.

A tentative phase diagram of the system NbO₂-Nb₂O₅ at high temperatures is shown in Fig. 5.

4. Defect Structure

For nonstoichiometric Nb₂O₅, the dependence of electrical conductivity on the oxygen partial pressure has been reported by many authors (13, 14, 25-29). The dependence is shown as follows:

$$\log \sigma = -\frac{1}{n} \log P_{O_2} + \sigma_0, \quad (1)$$

where P_{O_2} is the oxygen partial pressure, σ is the electrical conductivity, and σ_0 is the conductivity at 1 atm of oxygen pressure. The values of n have been reported as

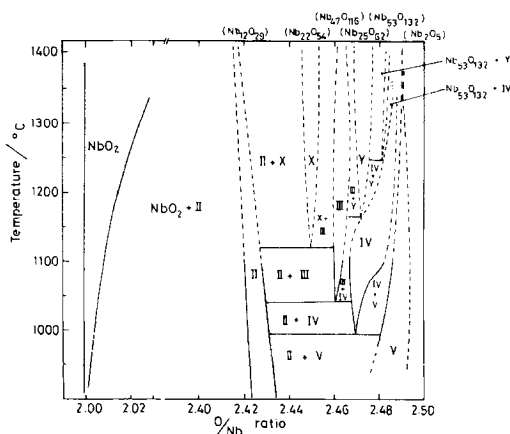


FIG. 5. Tentative phase diagram of the system of Nb-O at high temperatures.

follows: $n = 4.2$ in the oxygen pressure range from 0.95 to 0.002 atm at 680-770°C by Greener *et al.* (26), $n = 4.2$ in the oxygen pressure range 1-0.001 atm and $n = 6$ in the lower oxygen partial pressures in the mixtures of CO and CO₂ at 750-1200°C by Kofstad (25), $n = 4$ in the oxygen pressure range 1-0.005 atm at 900-1400°C by Greener *et al.* (27), $n = 4-4.3$ in the oxygen pressure range 1-10⁻⁶ atm at 800-1350°C by Chen and Swalin (28), $n = 4$ in the oxygen pressure range 1-10⁻¹⁶ atm at 909°C by Sheasby *et al.* (29), $n = 5.2$ in rather low oxygen pressure with mixtures of CO and CO₂ at 900-1300°C by Wimmer and Tripp (14), and $n = 6$ in the oxygen pressure range 10⁻¹⁰-10⁻¹³ atm at 1100°C and $n = 4$ in the range above 10⁻⁵ atm by Marucco (12). Based on the experimental results, doubly charged oxygen vacancies $V_O^{\bullet\bullet}$ were proposed by Kofstad (25, 30, 31) as the predominant defects in the region with small deviation from stoichiometry, and doubly charged interstitial niobium ions $Nb_i^{\bullet\bullet}$ for larger deviation from stoichiometry. Niobium interstitials $Nb_i^{\bullet\bullet}$ as defects were also proposed by Delmaire *et al.* (13) to interpret $n = 4.6-5$ at oxygen pressures down to the two-phase boundary with NbO₂ at

1000–1200°C. These dependences reported previously were obtained mostly without regard to the presence of intermediate phases, so it is necessary to determine the dependence for each phase.

a. In the nonstoichiometric region of Nb_2O_5 . In this region, $n = 4.2$ – 4.8 was obtained at 1010–1300°C as shown in Fig. 1. These n values can be interpreted by mixing oxygen vacancies with single ($n = 4$) and double ($n = 6$) charge, or by mixing the niobium interstitials with different charges. Considering the results obtained recently with the use of high-resolution electron microscopy (32–34), the mixing of oxygen vacancies is likely to exist as the defect structure in the nonstoichiometric region of Nb_2O_5 .

b. In region V. This region, as mentioned already, is considered to be a domain in which different kinds of defects are formed in Nb_2O_5 , and n varies with temperature: 7.8 at 1010°C, 5.8 at 1060°C, 5.7 at 1110°C, 5.1 at 1200°C, and 4.7 at 1300°C. Phase IV which is located at the oxygen-deficient side of region V is considered to have a similar structure to $Nb_{53}O_{132}$. The structure of $Nb_{53}O_{132}$ is known as a regular arrangement consisting of α - Nb_2O_5 ($N = Nb_{28}O_{70}$) and $Nb_{25}O_{62}$ with ratio Nb_2O_5 to $Nb_{25}O_{62}$ unity. An excess of Nb_2O_5 or $Nb_{25}O_{62}$ forms the defects (Wadsley defect) in $Nb_{53}O_{132}$. A similar mechanism of formation of defects can be expected in region V, where Wadsley defect is either $Nb_{25}O_{62}$ or $Nb_{53}O_{132}$ (a mixture of $Nb_{25}O_{62}$ and $Nb_{28}O_{70}$).

To Wadsley defects, Kikuchi and Goto (35) applied the same treatment as to the point defects and evaluated the value of n . Following their treatment, the values of n obtained in this study may be explained by assuming that the defect structure of region V consists of $Nb_{25}O_{62}$ type Wadsley defect and singly charged oxygen vacancy. However the quantitative discussion on this kind of defect is difficult since its structure

is complex and the interaction between defects is not negligible.

c. In the intermediate phases. Phase IV shows the different values of n at various temperatures: $n = 5.4$ at 1060°C, 5.2 at 1110°C, 2.0 at 1200°C, and 3.8 at 1300°C. The values of n at rather lower temperatures (1060 and 1110°C) may be interpreted by a similar complex defect model consisting of point defects and $Nb_{22}O_{54}$ type Wadsley defects. However, for values of n at higher temperatures (1200 and 1300°C), an explanation based on other defect structure seems to be necessary.

Phase III shows $n = 5.4$ at 1110°C, 8.0 at 1200°C, and 16 at 1300°C. These values may be explainable by a complex defect model consisting of singly charged oxygen vacancy and $Nb_{22}O_{54}$ type Wadsley defect.

Phase X is considered to correspond to $Nb_{22}O_{54}$, and the values of n are obtained as 2.9 at 1200°C and 8.3 at 1300°C. The defect structure-conduction mechanism to interpret this result is not simple.

In phase II, we obtained $n = 4.9$ at 1060°C and 5.5 at 1110°C, which may also be interpreted by a mixing model of singly charged oxygen vacancy and doubly charged oxygen vacancy: 38% of $[V_O^{\cdot\cdot}]$ at 1060°C and 69% of $[V_O^{\cdot\cdot}]$ at 1110°C.

d. In the NbO_2 phase. A semiconductor–metal transition of NbO_2 has been reported by several authors (36–39) at about 800°C. Because the temperature range where the present study was carried out is above the transition temperature, the electrical conductivities measured in this study show metallic conduction, independent of oxygen activity, in agreement with the results by Roberson and Rapp (40).

Acknowledgments

The authors thank Mr. H. Watanabe and Mr. T. Imura of the work shop center in Nagoya University for their experimental support. A part of this work was supported by Science Research Grant of the Ministry of Education.

References

1. G. BRAUER, *Z. Anorg. Allg. Chem.* **248**, 1 (1941).
2. R. N. BLUMENTHAL, J. B. MOSER, AND D. H. WHITMORE, *J. Amer. Ceram. Soc.* **48**, 617 (1965).
3. R. NORIN AND A. MAGNELI, *Naturwissenschaften* **47**, 354 (1960).
4. L. M. KOVBA, V. K. TRUNOV, AND Z. Ya. Pol'schikova, *Izv. Ak. Nauk SSSR Neorg. Mat.* **3**, 403 (1967).
5. A. BRUDEZE, E. V. TKACHENKO, AND K. ABBATTISTA, *Izv. Ak. Nauk SSSR Neorg. Mat.* **5**, 1957 (1969).
6. K. ABBATTISTA, G. CHIANTARETTO, AND E. V. TKACHENKO, *Atti Accad. Sci. Torino. I. Cl. Sci. Fis. Mat. Natur.* **102**, 865 (1967-1968).
7. H. SCHÄFER, D. BERGNER, AND R. GRUEHN, *Z. Anorg. Allg. Chem.* **365**, 31 (1969).
8. S. KIMURA, *J. Solid State Chem.* **6**, 438 (1973).
9. K. M. NIMMO AND J. S. ANDERSON, *J. Chem. Soc., Dalton* 2328 (1972).
10. J. F. MARUCCO, *Compt. Rend. Acad. Sci. Paris* **275**, 1391 (1972).
11. J. F. MARUCCO, *J. Solid State Chem.* **10**, 211 (1974).
12. J. F. MARUCCO, *J. Chem. Phys.* **70**, 644 (1979).
13. J. P. DELMAIRE, N. WALLET, AND A. DUQUESNOY, *Compt. Rend. Acad. Sci. Paris* **264**, 1290 (1967).
14. J. M. WIMMER AND W. C. TRIPP, ARL 73-0157 (1973).
15. T. ISHII, K. NAITO, AND K. OSHIMA, *J. Nuclear Mat.* **35**, 335 (1970).
16. "JANAF Thermochemical Tables" (D. R. Stall, Ed.). Dow Chemical Co., Midland, Mich. (1965).
17. K. NAITO, unpublished.
18. J. F. BAUMARD, D. PANIS, AND A. M. ANTHONY, *J. Solid State Chem.* **20**, 43 (1977).
19. R. GRUEHN AND R. NORIN, *Z. Anorg. Allg. Chem.* **355**, 176 (1967).
20. A. MAGNELI, G. ANDERSSON, AND G. SUNBVIST, *Acta Chem. Scand.* **9**, 1402 (1955).
21. N. TERAQ, *Japan. J. Appl. Phys.* **2**, 565 (1963).
22. R. NORIN, *Acta Chem. Scand.* **20**, 871 (1966).
23. R. GRUEHN AND R. NORIN, *Z. Anorg. Allg. Chem.* **367**, 209 (1969).
24. F. HOLTZBERG, A. REISMAN, M. BERRY, AND M. BERKENBLIT, *J. Amer. Chem. Soc.* **79**, 2039 (1957).
25. P. KOFSTAD, *J. Phys. Chem. Solids* **23**, 1571 (1962).
26. E. H. GREENER, D. H. WHITMORE, AND M. E. FINE, *J. Chem. Phys.* **34**, 1017 (1961).
27. E. H. GREENER, G. A. FEHR, AND W. M. HIRTHE, *J. Chem. Phys.* **38**, 133 (1963).
28. W. K. CHEN AND R. A. SWALIN, *J. Phys. Chem. Solids* **27**, 57 (1966).
29. J. S. SHEASBY, W. W. SMELTZER, AND A. E. JENKINS, *J. Electrochem. Soc.* **115**, 338 (1968).
30. P. KOFSTAD, "Nonstoichiometry, Diffusion and Electrical Conductivity in Binary Metal Oxide," p. 182. Wiley-Interscience, New York (1972).
31. P. KOFSTAD, *J. Less-Common Metals* **14**, 153 (1968).
32. J. S. ANDERSON, J. M. BROWNE, AND J. L. HUTCHISON, *J. Solid State Chem.* **5**, 419 (1972).
33. S. IJIMA, *Acta Cryst.* **A29**, 18 (1973).
34. S. IJIMA, S. KIMURA, AND M. GOTO, *Acta Cryst.* **A30**, 251 (1974).
35. T. KIKUCHI AND M. GOTO, *J. Solid State Chem.* **16**, 363 (1976).
36. R. F. JANNICK AND D. H. WHITMORE, *J. Phys. Chem. Solids* **27**, 1183 (1966).
37. K. SAKATA, *J. Phys. Soc. Japan* **26**, 867 (1969).
38. C. N. R. RAO, G. R. RAO, AND G. V. S. RAO, *J. Solid State Chem.* **6**, 340 (1973).
39. G. BELANGER, J. DESTRY, G. PERLUZZO, AND P. M. RACCAH, *Canad. J. Physics* **52**, 2272 (1974).
40. J. A. ROBERSON AND R. A. RAPP, *J. Phys. Chem. Solids* **30**, 1119 (1969).